Photophysics of mixed-ligand polypyridyl ruthenium(II) complexes immobilised in silica sol–gel monoliths

Karen F. Mongey,[a] Johannes G. Vos,*[a] Brian D. MacCraith,[b] Colette M. McDonagh,[b] Colin Coates[c] and John J. McGarvey[c]

[a]*School of Chemical Sciences, Dublin City University, Dublin 9, Ireland*
[b]*School of Physical Sciences, Dublin City University, Dublin 9, Ireland*
[c]*School of Chemistry, Queens University, Belfast BT9 5AG, Northern Ireland*

A series of compounds $[Ru(bpy)_{3-x}(dpp)_x]^{2+}$ (bpy = 2,2′-bipyridyl, dpp = 4,7-diphenyl-1,10-phenanthroline) have been synthesised and physically immobilised in silica sol–gel monoliths. Transient resonance-Raman studies show that for the immobilised mixed-ligand complexes, as in solution, the emitting (^{3}MLCT) state is dpp based. The resonance-Raman evidence also suggests that the structure of this state is the same in both environments. The emission lifetimes of the immobilised complexes cannot be analysed as single exponential decays and the values obtained are dependent on the initial pH of the sol–gel. The temperature-dependent emission behaviour of the compounds is substantially changed upon immobilisation in the sol–gel. Both the variation of the emission lifetime and energy are significantly different from that observed for the solution-based species. For the bpy containing complexes no evidence is obtained for the population of the photoactive ligand field state, whereas for the complex $[Ru(dpp)_3]^{2+}$ population of this state is observed. The relevance of these observations for the design of optical sensors for oxygen is discussed.

In the last two decades, there has been continued interest in the investigation of the photophysical and photochemical properties of ruthenium(II) polypyridyl complexes. They have attracted the attention of several research groups because of a unique combination of ground- and excited-state properties. The prototype of these complexes, $[Ru(bpy)_3]^{2+}$ (bpy = 2,2′-bipyridyl), has been used as a photoluminescent compound, an excited-state reactant in energy and electron transfer processes, an excited-state product in chemiluminescent and electrochemiluminescent reactions, and also a mediator in the conversion of light and chemical reactions.[1–9]

$[Ru(bpy)_3]^{2+}$ exhibits an intense absorption band at approximately 452 nm which has been assigned to a metal-to-ligand charge transfer (^{1}MLCT). Fast intersystem crossing occurs from this level to the triplet MLCT state (^{3}MLCT). Emission from the triplet state to the ground state or radiationless deactivation to the ground state are observed. In addition, population of a metal-centred (^{3}MC) excited state causes cleavage of a Ru—N bond, leading to photosubstitution.

In general, the study of the photophysical pathways of ruthenium(II) polypyridyl complexes in solids has progressed at a much slower pace than in solution. However, because of the proliferation of practical applications upon incorporation of such complexes into a membrane or solid matrix, their photophysics in a solid environment now presents a formidable challenge to the material scientist. For example, an extensive chemistry dealing with the immobilisation of ruthenium(II) polypyridyl complexes in glass-like matrices such as sol–gel derived glasses and Vycor glass has recently emerged.[10–13] This work is strongly motivated by the possible application of such modified glasses as sensors for oxygen.[14–16] The photophysical aspects of such materials are by no means straightforward. In contrast to more conventional homogeneous luminescent materials, these supports are frequently heterogeneous on a microscopic scale, giving rise to complex and poorly characterised decay kinetics. This complexity may result in obscure sensor response. In effect, heterogeneity makes the analysis of photochemical and photophysical data much more complex than in fluid systems.

Here, we report the immobilisation of a series of compounds, $[Ru(bpy)_{3-x}(dpp)_x]^{2+}$ (dpp = 4,7-diphenyl-1,10-phenanthroline) in silica monoliths prepared *via* the sol–gel process, and their subsequent characterisation using a number of spectroscopic techniques. The optically transparent nature of the silica gel matrix ensures that optical techniques involving the interaction of photons with the trapped ruthenium(II) complexes can be used to study the photophysical properties of these encapsulated species. Analysis of the temperature-dependent emission wavelength and luminescent lifetime of the immobilised complexes was carried out in an effort to more precisely understand the the nature of the photophysics of these complexes in the solid state.

Experimental

Materials

All synthetic reagents and solvents were of commercial grade and no further purification was employed. The complexes $[Ru(bpy)_3](PF_6)_2$,[17] $[Ru(dpp)_3](PF_6)_2$,[18] $[Ru(bpy)_2(dpp)](PF_6)_2$[19] and $[Ru(dpp)_2(bpy)](PF_6)_2$,[19] were synthesised according to general literature procedures. The purity of the complexes was established using HPLC[20] and proton NMR techniques.

Preparations

Monolithic sol–gel samples were prepared by the hydrolysis and condensation of tetraethoxysilane (TEOS) in an ethanol solution. A water : TEOS ratio of 4 : 1 was used.

To a mixture of 3.6 g (0.2 mol) of water (adjusted to the appropriate pH using conc. HCl) and 13.8 g (0.3 mol) of ethanol (containing the desired dopant complex), 10.4 g (0.05 mol) of TEOS was added dropwise. The mixture was stirred for 1 h in a sealed beaker before pouring into a plastic cell suitable for spectroscopic measurements. The plastic cell was covered to allow gelation and ageing to occur in a closed environment at a temperature of 50 °C. The initial concentration of the complexes in the sols was 10^{-5} M. After ageing (500 h) the sample lid was pierced to allow the evaporation of excess solvent for 300 h. Throughout the sol–gel process

samples were stored at 50 °C. The time required to reach the gel point was found to depend greatly on the initial pH employed. At pH 1 gelation times were typically 350 h, while at pH 5 a period of 50 h was sufficient.[21] The undoped gels display high optical transparency in the visible region.

Instrumentation

UV–VIS spectra were obtained using a Shimadzu 3100 UV–VIS/NIR spectrophotometer. Solid sol–gel samples were measured with a UV–VIS/NIR integrating sphere attachment which employs the diffuse reflectance technique.[22]

Emission spectra were carried out with an LS50B spectrometer fitted with a Hamamatsu R928 red-sensitive detector. The spectra were not corrected for photomultiplier response. Measurements of the quantum yields of emission, Φ_{em}, were carried out using optically dilute samples as described by Demas and Crosby[23,24] and are accurate to $\pm 10\%$.

Emission spectra were determined as a function of temperature with a custom-built quartz sample holder in combination with a variable temperature liquid-nitrogen cryostat PE1704 equipped with a Thor 3030 temperature controller. Samples were degassed for 30 min under nitrogen prior to analysis. The absolute error on the temperature is estimated at ± 2 K. Emission lifetime measurements were carried out using a Q-switched Nd-YAG laser system (Quanta-Ray GCR2, pulse width 9 ns). The emission decay curves were analysed as single and double exponentials using standard methods.

Transient resonance-Raman (RR) spectra in solution were recorded in acetonitrile (*ca.* 10^{-4} mol dm^{-3}). For resonance-Raman measurements samples of the complex in the sol–gel glass in the form of small pieces, 0.5–2 mm diameter, were packed into the bottom of a cylindrical cell which was spun at 100 rpm in the excitation laser beam. Spectra were acquired using a 180° scattering geometry on an EG&G OMA III multichannel detector. The excitation pulse energy at 355 nm was typically 3 mJ for the solution spectra and 4 mJ at the sol–gel sample. Ground-state RR spectra were recorded by means of CW excitation at 363.8 nm, also in a backscattering geometry using an Ar^+ laser (Spectra Physics Model 2025) and a CCD detector (Princeton Instruments Model LN/UV 1152) coupled to a Jobin-Yvon spectrograph (Model HR640). Typical laser power at the sample was 30 mW.

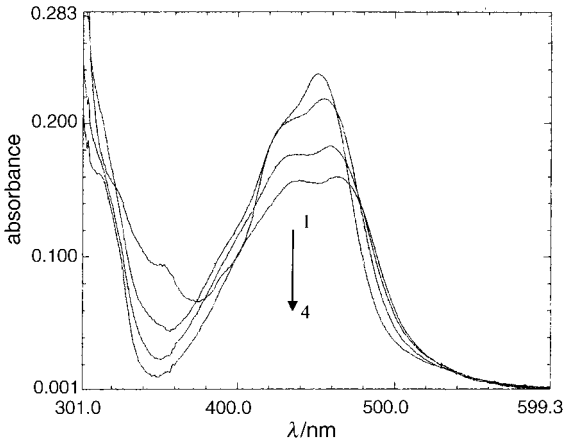

Fig. 1 Absorption spectra of $[Ru(bpy)_{3-x}(dpp)_x]^{2+}$ in ethanol: (1) $[Ru(bpy)_3]^{2+}$, (2) $[Ru(bpy)_2(dpp)]^{2+}$, (3) $[Ru(bpy)(dpp)_2]^{2+}$, (4) $[Ru(dpp)_3]^{2+}$

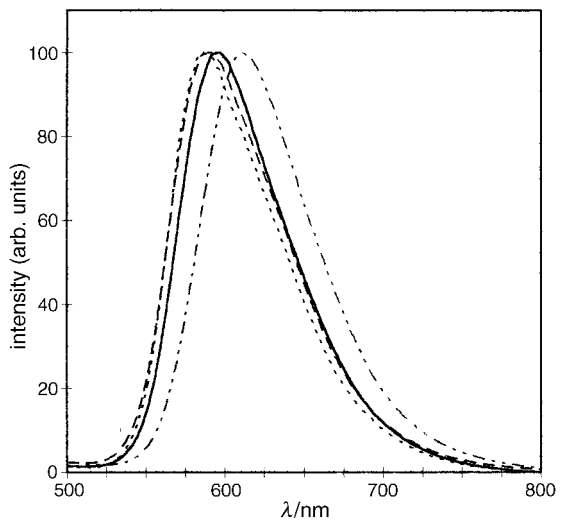

Fig. 2 Normalised emission spectra of $[Ru(bpy)_{3-x}(dpp)_x]^{2+}$ in xerogel prepared at pH 5 at room temperature. From left to right $[Ru(bpy)_3]^{2+}$, $[Ru(bpy)_2(dpp)]^{2+}$, $[Ru(bpy)(dpp)_2]^{2+}$, $[Ru(dpp)_3]^{2+}$.

Results

Electronic spectra

Fig. 1 shows the absorption spectra of the $[Ru(bpy)_{3-x}(dpp)_x]^{2+}$ series of compounds in the visible region in ethanol. The absorption features of the immobilised complexes are not significantly changed from those observed in solution. The emission data obtained in solution and in the sol–gel matrix are listed in Table 1. For the immobilised species, data are presented for each complex in two different sol–gel matrices; one prepared at an initial pH of 1 and a second one at pH 5. A typical set of emission spectra obtained at room-temperature is given in Fig. 2. Table 2 reports the photophysical rate

Table 1 Excited-state properties of $[Ru(bpy)_{3-n}(dpp)_n]^{2+}$ in solution and in the final xerogel

complex	medium	$\lambda_{max}{}^a$/nm	$\lambda_{max}{}^b$/nm	$\tau^{a,c}$/ns	$\tau^{b,c}$/ns
$[Ru(bpy)_3]^{2+}$	solution	611	580	[700] 280	4500
	gel pH 1	597	579	1110(70), 470(30)	4490(75), 1590(25)
	gel pH 5	588	576	2100(80), 660(20)	4450(85), 1800(15)
$[Ru(bpy)_2(dpp)]^{2+}$	solution	612	588	[1970] 290	8830
	gel pH 1	600	585	920(70), 220(30)	8750(65), 2770(35)
	gel pH 5	590	582	2780(80), 800(20)	8600(80), 2590(20)
$[Ru(bpy)(dpp)_2]^{2+}$	solution	613	592	[4100] 295	9420
	gel pH 1	604	594	720(75), 180(25)	9500(70), 2900(30)
	gel pH 5	598	597	3000(70), 600(30)	9550(80), 2705(20)
$[Ru(dpp)_3]^{2+}$	solution	612	597	[4890] 290	9640
	gel pH 1	611	596	2100(65), 520(35)	9750(70), 2005(30)
	gel pH 5	612	597	1200(70), 300(30)	9800(80), 2435(20)

[a]Room-temperature measurements were obtained in aerated conditions. The values in square brackets for the solutions indicate the lifetime of the complex in deaerated solution. [b]Measurements were carried out at 77 K. For solution values, the solvent employed was ethanol–methanol (4:1, v/v). [c]Values in parentheses are pre-exponential factors for the two different lifetime components in the gel matrix given in %.

Table 2 Excited-state decay parameters of $[Ru(bpy)_{3-n}(dpp)_n]^{2+}$ series of complexes in ethanol solution

complex	k^r/s^{-1}	k^{nr}/s^{-1}	k_0/s^{-1}	Φ_{em}
$[Ru(bpy)_3]^{2+}$	2.3×10^4	2.0×10^5	2.2×10^5	1.60×10^{-2}
$[Ru(bpy)_2(dpp)]^{2+}$	7.1×10^3	1.1×10^5	1.1×10^5	1.40×10^{-2}
$[Ru(bpy)(dpp)_2]^{2+}$	3.5×10^3	1.0×10^5	1.1×10^5	1.50×10^{-2}
$[Ru(dpp)_3]^{2+}$	3.1×10^3	1.0×10^5	1.0×10^5	1.51×10^{-2}

constant k_0 ($=k^r+k^{nr}$), which consists of a radiative (k^r) and a non-radiative component (k^{nr}) estimated using eqn. (1) and (2) below, and the values obtained for the emission quantum yield Φ_{em}. The emission quantum yields for the immobilised complexes could not be calculated due to the fractured nature of the solid gel samples.

$$k^r = \Phi_{em}/\tau \quad (1)$$

$$k^{nr} = (1/\tau_{77K}) - k^r \quad (2)$$

In all cases the emission decay curves of the solid gel samples show a non-single exponential behaviour and a double exponential model was employed. The lifetimes obtained in this manner together with their weighting in % are given in Table 1.

Resonance-Raman spectra

Transient resonance-Raman spectra of $[Ru(bpy)(dpp)_2]^{2+}$ have been recorded using pulsed laser excitation at 355 nm both in acetonitrile solution and in a pH 5 gel (Fig. 3). The spectra are compared in Fig. 4 with the corresponding ground-state RR spectra recorded using continuous wave excitation at 363.8 nm.

Temperature dependence

The variation of the emission energy with temperature for $[Ru(bpy)_3]^{2+}$, $[Ru(bpy)(dpp)_2]^{2+}$ and $[Ru(dpp)_3]^{2+}$ both in solution and in the sol–gel is shown in Fig. 5–7. The temperature dependence of the lifetime of each of the four complexes was also investigated. It was found for the immobi-

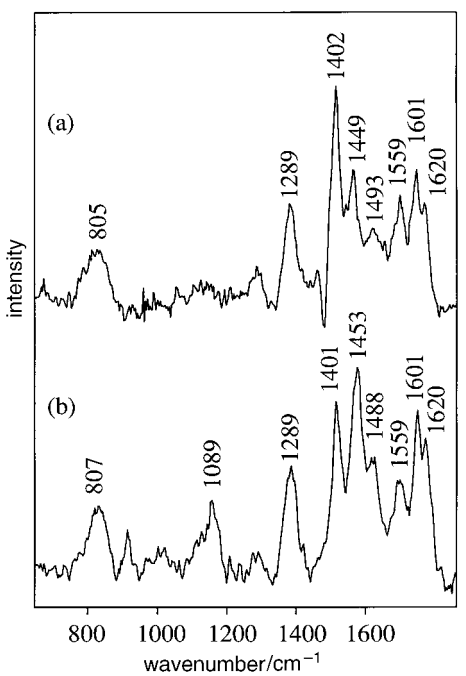

Fig. 3 Transient resonance-Raman spectra of $[Ru(bpy)(dpp)_2]^{2+}$ in acetonitrile generated with pulsed excitation at 355 nm: (a) in acetonitrile; (b) in a sol–gel matrix prepared at pH 5. Pulse energies 3 and 4 mJ, respectively.

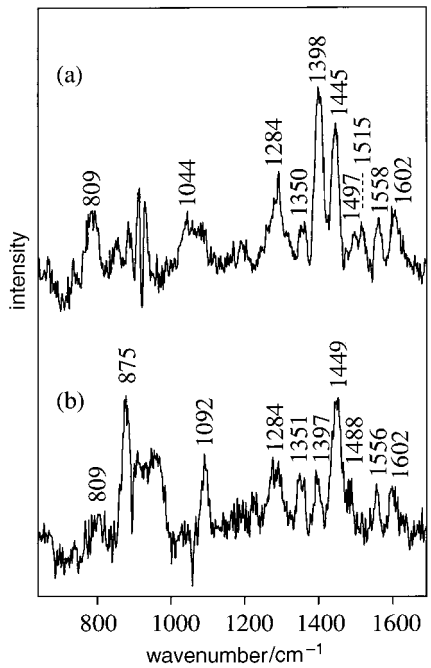

Fig. 4 Ground-state resonance-Raman spectra of $[Ru(bpy)(dpp)_2]^{2+}$, generated using CW excitation at 363.8 nm (Ar^+ laser): (a) in acetonitrile, (b) in a sol–gel matrix prepared at pH 5. Laser power at sample *ca.* 30 mW in both cases.

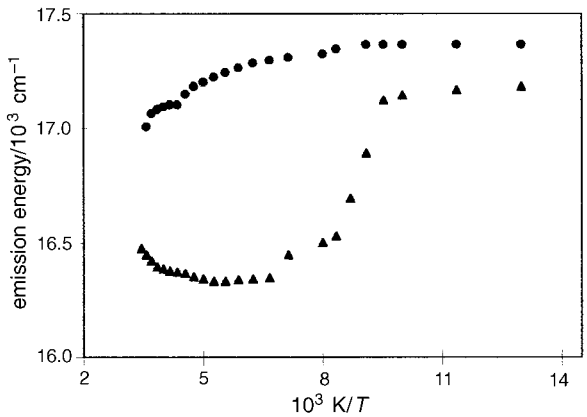

Fig. 5 Shift of the emission maxima with temperature for $[Ru(bpy)_3]^{2+}$ in solution (▲) and in a sol–gel prepared at pH 5 (●) in the temperature range 77–300 K

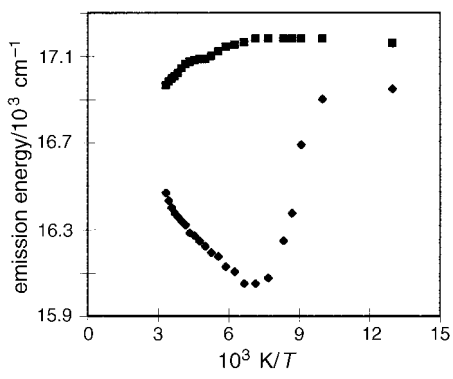

Fig. 6 Shift of the emission maxima with temperature for $[Ru(bpy)_2(dpp)]^{2+}$ in solution (◆) and in a sol–gel prepared at pH 5 (■) in the temperature range 77–300 K

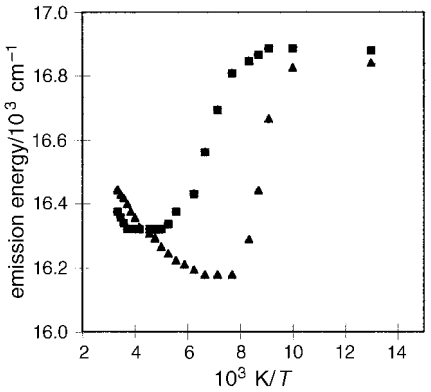

Fig. 7 Shift of the emission maxima with temperature for $[Ru(dpp)_3]^{2+}$ in solution (▲) and in a sol–gel prepared at pH 5 (■) in the temperature range 77–300 K

lised complexes, that both lifetime components for any one sol–gel sample exhibited a similar trend. Fig. 8 shows the temperature-dependent behaviour of both lifetime components for $[Ru(bpy)_3]^{2+}$ in a sol–gel monolith. We have therefore used only the results obtained from the analysis of the longer lived main component. The results obtained for this component for the four different compounds are shown in Fig. 9. The temperature dependence of the lifetimes in solution and the solid matrix has been used to determine the activation param-

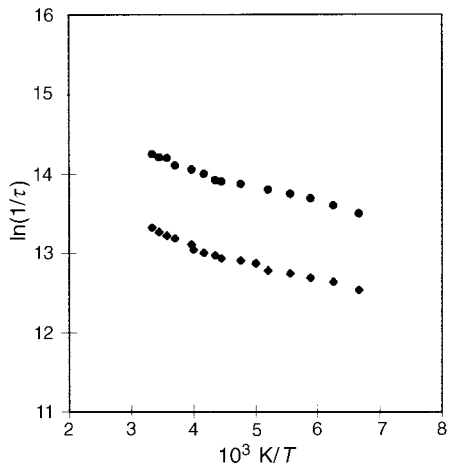

Fig. 8 Temperature dependence of the long (●) and short (◆) lifetime components of $[Ru(bpy)_3]^{2+}$ in xerogel prepared at pH 1

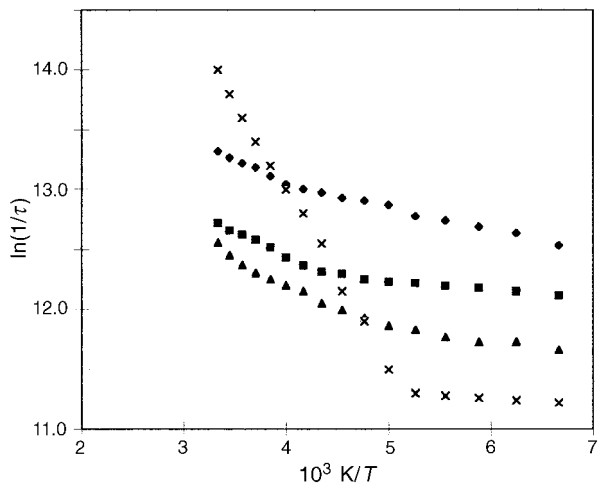

Fig. 9 Temperature dependence for the luminescence lifetime of (◆) $[Ru(bpy)_3]^{2+}$, (●) $[Ru(bpy)_2(dpp)]^{2+}$, (▲) $[Ru(bpy)(dpp)_2]^{2+}$, (×) $[Ru(dpp)_3]^{2+}$ in a sol–gel matrix prepared at pH 5

eters for deactivation of the emitting ^{3}MLCT level. The activation energies and pre-exponential parameters A as obtained from eqn. (3)

$$1/\tau = k_0 + A\exp\left(\frac{-\Delta E}{RT}\right) \quad (3)$$

are given in Table 3. In solution, measurements were confined to the temperature range above 150 K in order to minimise possible complications associated with the freezing of the solvent.

The analysis of the data obtained is based on the following model. Activation parameters obtained for ^{3}MLCT emission of ruthenium complexes usually fall into one of two categories:[9,13] (*a*) small activation energies ($<800\ cm^{-1}$) and low prefactors ($<10^9\ s^{-1}$) or (*b*) large activation energies ($>2000\ cm^{-1}$) and large prefactors ($>10^{11}\ s^{-1}$).

Case (*a*) has been ascribed to the population of a ^{3}MLCT state which lies approximately $800\ cm^{-1}$ above the lowest lying emitting ^{3}MLCT state. For case (*b*) the activated process has been ascribed to population of the ^{3}MC state. If relaxation of the ^{3}MC state is rapid relative to crossover from the ^{3}MC state back to the ^{3}MLCT state, the measured ΔE represents the activation energy for ^{3}MLCT–^{3}MC internal conversion (case *b*1). Since in this case there is a strong coupling a prefactor in the range 10^{13}–$10^{14}\ s^{-1}$ is expected. If on the other hand the ^{3}MLCT and ^{3}MC states are in equilibrium and the deactivation of the ^{3}MC state occurs *via* a non-activated process, the measured activation energy corresponds approximately to the energy gap between the two states (case *b*2). This will lead to a smaller activation energy being obtained. In this case the prefactor for the process will generally be lower than that for the case of rapid ^{3}MC-state decay (10^{10}–$10^{12}\ s^{-1}$). Variations between parameters, in particular k_0, displayed in Tables 2 and 3 and those in the literature[9,24,25] reflect the limitations imposed by fitting a restricted number of data points over a small temperature range. However, overall the results obtained compare well and the comparisons made below are considered to be valid. For the solvent system employed here [ethanol–methanol (4:1, v/v)], solvent melting occurs in the 100–120 K temperature region. Kinetic parameters were derived by fitting data obtained at temperatures above this transition region.

Discussion

Electronic spectra

In the sol–gel matrix, each member of this series of ruthenium compounds retains its typical UV–VIS spectral features and the compounds are luminescent at room temperature and at 77 K. The similarity of the absorption spectra obtained for the compounds in solution and when immobilised, suggests that no substantial change in the energy gap between the ground state and the ^{1}MLCT state occurs upon incorporation into the sol–gel matrix. At room temperature there are small but significant differences in the emission maxima of the complexes after immobilisation in the solid matrix. Table 1 shows that for the bpy-containing complexes the shifts observed are more significant than for $[Ru(dpp)_3]^{2+}$, for which the emission energy is insensitive to incorporation in the gel and also to its intitial pH. The shifts to higher energy observed for the $[Ru(bpy)_3]^{2+}$ can be explained by the destabilisation of the ^{3}MLCT state because of the reduced mobility of dipoles in the solid matrix.[26,27] Clearly this effect is much less significant for the tris dpp complex.

The data presented in Table 1 indicate that the observed excited-state decay lifetime of all four complexes of this series increases upon incorporation into the sol–gel (as compared to the room-temperature aerated solution value). The extent of this increase appears to depend very much on the complex in

Table 3 Kinetic parameters k_0, A and ΔE, for the decay of the MLCT states of $[Ru(bpy)_{3-x}(dpp)_x]^{2+}$ series of complexes in ethanol–methanol (4:1, v/v) solution and in the sol–gel matrix

complex	matrix	k_0/s^{-1}	A/s^{-1}	$\Delta E/cm^{-1}$
$[Ru(bpy)_3]^{2+}$	EtOH–MeOH	4.5×10^5	1.4×10^{14}	3900
	cell/acetate[a]	1.00×10^7	1.70×10^7	810
	gel pH 1	2.3×10^5	1.2×10^7	740
	gel pH 5	3.0×10^5	9.1×10^6	660
$[Ru(bpy)_2(dpp)]^{2+}$	EtOH–MeOH	3.4×10^5	0.70×10^{13}	2900
	gel pH 1	1.59×10^5	2.75×10^8	995
	gel pH 5	1.9×10^5	1.79×10^7	940
$[Ru(bpy)(dpp)_2]^{2+}$	EtOH–MeOH	1.6×10^5	0.65×10^{13}	2950
	gel pH 1	3.34×10^5	3.4×10^7	800
	gel pH 5	1.5×10^5	2.6×10^6	660
$[Ru(dpp)_3]^{2+}$	EtOH–MeOH	1.4×10^5	3.2×10^{12}	2675
	gel pH 1	1.27×10^5	3.0×10^{12}	2700
	gel pH 5	1.1×10^5	1.3×10^{12}	2520

[a]From ref. 5.

question. This is again explained by the rigid nature of the sol–gel matrix, which in addition to a destabilisation of the emitting state as outlined above, will also cause a decrease in the nonradiative decay k^{nr} because of restricted molecular motion of the immobilised complex. The diffusion of oxygen will also be limited by the matrix. While other researchers have used models such as multiexponential fits and statistical distributions to fit the decay lifetime data for immobilised ruthenium complexes,[11,28,29] we have employed a double exponential method as a more simple yet adequate approach.

The lifetime of the emitting state of the immobilised complexes is expected to be influenced both by the size of the pores and by the charge of the surface of the sol–gel matrix. Table 1 shows that the lifetimes obtained at room temperature are dependent on the pH at which the gel was prepared. The three bpy containing compounds behave similarly and have longer lifetimes in gels prepared at pH 5. On the other hand the tris(dpp) complex shows enhanced lifetimes in pH 1 gels. This observation indicates that the tris(dpp) complex behaves rather differently from the bpy containing species.

It is well known that at pH 1 the silica sol–gel surface is positively charged, while in gels prepared at pH 5 a negatively charged surface is expected.[26] Furthermore at pH 5 larger pores are expected in the gel matrix.[30–32] With small pores the rigidity of the medium around the emitting species is increased and as a result the lifetime is expected to be longer. It also seems reasonable to assume that the excited state, which formally contains a negatively charged polypyridyl ligand, will interact less strongly with a negatively charged surface than with a positively charged one. The lifetimes obtained suggest that the emitting behaviour of the bpy containing compounds is mainly dependent on the charge of the surface, while the tris(dpp) complex is isolated from the charged surface but is affected by the pore size. This suggests a relatively shielded excited-state for the tris(dpp) complex. So, while the electronic properties of the immobilised $[Ru(bpy)_3]^{2+}$, $[Ru(bpy)_2(dpp)]^{2+}$ and $[Ru(bpy)(dpp)_2]^{2+}$ complexes appear to be modified by the electrostatic interaction between the complex and the surface silanols, the $[Ru(dpp)_3]^{2+}$ complex appears to be relatively unaffected by the sol–gel cage. Considering the presence of the large phenyl rings outside the phenanthroline centre this reduced influence of the surface is not unexpected.

Resonance-Raman spectra

In $[Ru(bpy)_3]^{2+}$ the lowest excited state is ^{3}MLCT in nature and is localised on the bipyridyl ligands.[33] However in mixed-ligand complexes of the type $[Ru(bpy)_2(dpp)]^{2+}$, the emitting state can be bpy or dpp based. In a recent study by Kumar and co-workers[34,35] it was shown that the excited-state resonance-Raman spectrum of $[Ru(bpy)_2(dpp)]^{2+}$ is dominated by features characteristic of the $dpp^{\cdot -}$ ligand. It has therefore been assumed that the emitting state in solution is dpp based. The transient RR spectra recorded in this present study for $[Ru(bpy)(dpp)_2]^{2+}$ in solution (Fig. 3) are in line with this assignment. Strongly enhanced bands are observed at 1208, 1289, 1401, 1449,1601 and 1620 cm^{-1} which are characteristic vibrations for the dpp^- moiety.[34,35] In addition, the emission lifetimes observed for the mixed-ligand complexes are consistent with such an assignment. The values obtained in deaerated solutions show a large increase upon the introduction of a dpp ligand. Interestingly the lifetime in aerated solutions for all four complexes is almost constant, an indication that dpp complexes are more efficiently quenched by oxygen. The excited-state decay parameters given in Table 2 do not yield further information about the nature of the excited state. There is no clear trend upon the addition of dpp ligands, although all rate constants decrease somewhat in dpp complexes.

The vibrational modes in the excited-state RR spectrum of $[Ru(bpy)(dpp)_2]^{2+}$ recorded in the sol–gel (Fig. 3) are at virtually identical frequencies to those that appear in the corresponding spectrum of the complex recorded in solution indicating that in the solid matrix the the emitting state is firmly dpp based. An examination of the spectra shows however, there are differences in relative intensity between the two sets of bands (showing enhanced vibrations at 1208, 1289, 1401, 1454, 1559, 1601 and 1620 cm^{-1}). This point is considered later.

Temperature-dependent studies

Fig. 5–7 show the temperature dependence of the emission energy of three of the complexes both in alcohol solution and in a sol–gel matrix in the temperature range 77–300 K. As shown in Fig. 5, during the melting of the 4:1 ethanol–methanol solvent, the emission maximum of $[Ru(bpy)_3]^{2+}$ moves towards lower energies as expected. Upon incorporation into the sol–gel matrix the glass-to-fluid transition is effectively removed. The emission energy remains largely unchanged suggesting that no major changes are occurring in the gel structure with increasing temperature. In solution, a blue shift in the emission energy occurs at higher temperatures. It is not clear why such a shift occurs, but it is thought to be associated with the population of higher lying ^{3}MLCT levels which are higher in energy than the lowest lying ^{3}MLCT level. Such an increase in the emission energy is however not observed in the gel. Similar results are shown in Fig. 3 for $[Ru(bpy)_2(dpp)]^{2+}$.

The behaviour observed for $[Ru(dpp)_3]^{2+}$ is significantly different (Fig. 7). A decrease in emission energy similar to the one observed in solution upon melting of the solvent is observed for the immobilised compound but the temperature where this transition occurs is higher at *ca.* 140 K than in

ethanol–methanol (*ca.* 110 K). A significant decrease in the emission energy of the immobilised complex is observed as the temperature is raised, from *ca.* 16 830 cm^{-1} at 140 K to 16 320 cm^{-1} at 250 K. Although not as pronounced as the decrease observed for this complex in solution, the shift of the emission energy is nevertheless much greater than that observed for any of the bpy complexes in this series. The temperature-dependent behaviour of the emission energy of the immobilised $[Ru(dpp)_3]^{2+}$ suggests that even in the xerogel state, sufficient solvent molecules remain within the porous structure, and that the $[Ru(dpp)_3]^{2+}$ molecules are in fact solvated to a large extent. This in turn suggests that 140 K corresponds to the melting point of the solvent within the sol–gel pores (*i.e.* water–ethanol). In agreement with this interpretation it is observed that the melting point of ethanol, the solvent used during the gel formation, is 156 K, well within the temperature range where the decrease in emission energy and lifetime is observed for the tris(dpp) complex.

The excited-state kinetic parameters for the first three members of this series (namely $[Ru(bpy)_3]^{2+}$, $[Ru(bpy)_2(dpp)]^{2+}$ and $[Ru(bpy)(dpp)_2]^{2+}$) in the sol–gel matrix are clearly very different from the parameters in solution (see Table 3 and Fig. 9). The activation energies obtained for these compounds are between 600 and 900 cm^{-1} and are associated with prefactors of the order of 10^6–10^7 s^{-1}. This suggests that for these immobilised complexes population of a fourth ^{3}MLCT state rather than the ^{3}MC state occurs. There are a number of possible explanations for this behaviour which will be discussed in the following paragraph. The kinetic parameters for $[Ru(dpp)_3]^{2+}$ in the sol–gel matrix (*e.g.* $A = 1.27 \times 10^{12}$ s^{-1} and $\Delta E = 2520$ cm^{-1} in the sol–gel prepared at pH 5) are similar in value to those obtained in solution ($A = 3.2 \times 10^{12}$ s^{-1} and $\Delta E = 2675$ cm^{-1}). This suggests population of the metal based ^{3}MC level which indicates that, unlike the bpy based complexes, $[Ru(dpp)_3]^{2+}$ should be photolabile in the gel.

Previously it has been suggested that upon immobilisation of $[Ru(bpy)_3]^{2+}$ into a rigid matrix, expansion along the metal–ligand bond axes may be sufficiently costly energetically that access to the dd state is no longer feasible because of a significant increase of the energy of this level.[36,37] An alternative explanation for the observed temperature dependence of the emission involves 'rigid matrix effects'.[38,39] This interpretation maintains that the shapes of the potential-energy surfaces of the excited ^{3}MLCT and ^{3}MC states are perturbed in such a manner that surface crossing from the ^{3}MLCT to the ^{3}MC level, or from the ^{3}MC level to the ground state, can no longer occur in the temperature range studied. It is also possible that the sol–gel matrix induces some constraint on the complex and a decrease in ΔQ_e[40,41] (horizontal displacement of the equilibrium position of the potential-energy surfaces) for the ^{3}MC state relative to the ground state may result. As a consequence, the ground state and ^{3}MC state may be nested rather than strongly coupled as in solution and the decrease in ΔQ_e may reduce the surface crossing of the ^{3}MC and the ground-state potential surfaces so much so that deactivation of the ^{3}MC level by interaction with the ground state becomes very slow. Alternatively, a change in ΔQ_e may also result in the nesting of the ^{3}MLCT and the ^{3}MC potential-energy surfaces, reducing the probability of populating the ^{3}MC level from the emitting triplet state. In effect, upon immobilisation subtle changes in the equilibrium displacement of the excited states, rather than an increase in their energy, may give rise to the observed non-activated processes with low prefactors.

In the context of the foregoing discussion, it is interesting to consider the ground- and excited-state resonance-Raman spectra recorded for $[Ru(bpy)(dpp)_2]^{2+}$ both in solution and immobilised in the xerogel (Fig. 3 and 4). Comparison of the ground-state spectra recorded with 363.8 nm excitation (Fig. 4) shows features with nearly identical vibrational frequencies in both media but exhibiting different enhancement patterns in the two cases. These observations parallel those reported in several other studies of the ground-state RR spectra of ruthenium(II)bipyridyl-containing complexes in restrictive environments such as sol–gels[28] or zeolite cages[41] or adsorbed onto porous Vycor glass.[12,42] Since resonant-Raman frequencies are a property of the initial state of the electronic transition involved in the enhancement mechanism,[42] which in the CW-generated spectra under consideration is the ground state, the absence of frequency shifts has been taken to imply[41,42] that the structure of the ground state in the immobilised environment is similar to that observed in solution. On the other hand, it has been argued[12,42] that differences in the relative peak intensities between the two spectra indicate changes in the excited-state structure in the two media since the band intensity pattern is a property of the upper electronic state accessed through the resonant vibronic transition responsible for enhancement. In the various examples of ruthenium(II) polypyridyl complexes previously studied as well as that under consideration here, the upper state is ^{1}MLCT. However, in the present work we have also examined the RR spectra of the relaxed ^{3}MLCT excited state. It is quite clear from Fig. 3 that while the spectra recorded in the two media show virtually the same set of vibrational band frequencies, the intensity distributions are again different. If the argument applied above is also invoked here, the conclusion must be that the structures of the relaxed ^{3}MLCT states in both solution and in sol–gel matrix are the same, but the distinctive enhancement patterns suggest that the upper (terminal) states reached in the Raman excitation process are 'structurally' distinguishable. The degree of 'structural' change involved requires some consideration. Rather than speaking about major differences in excited-state structure between the two media, we prefer to think of the sol–gel environment as imposing some curtailment on the ligand distorting modes involved in the resonant transition, much as has been proposed recently by Fan and Gaffney[12] to account for changes in the relative intensities of ligand modes in $Ru(bpy)_3^{2+}$ adsorbed on Vycor glass. Ligand vibrational modes are obviously a dominant feature of the RR spectra generated from either the ground electronic state or from the 'thexi' ^{3}MLCT state since in both cases the transitions (which in formal terms take place to ^{1}MLCT ($Ru^{II} \rightarrow dpp$) and $^3\pi^*,\pi^*$ ($dpp^{\cdot -}$-centred) states respectively), involve distortions along ligand coordinates. It is not unreasonable to expect therefore that the RR intensity patterns might be similarly influenced in both instances by the constraints of the sol–gel environment, just as we observe here for the ground- and excited-state RR spectra of $[Ru(bpy)(dpp)_2]^{2+}$. The 'nascent' ^{1}MLCT populated by excitation from the ground state will relax *via* 'vibrational ladders' of excited species-sol–gel cage configurations towards the 'thexi' ^{3}MLCT state. (The scenario envisaged here bears a formal resemblance to that originally proposed by Adamson[43] to describe the relaxation of an initially populated Franck–Condon state of a metal complex *via* a succession of excited-state-solvent cage potential wells towards the thermally relaxed excited state.) In the present case, the thermally relaxed state ultimately attained is virtually the same as that reached in solution and would be expected to exhibit the same vibrational frequencies, as is indeed observed.

The question still remains as to why the $[Ru(dpp)_3]^{2+}$ immobilsed complex behaves in opposition to the other members in this series. We propose two possible explanations for the behaviour observed for this different behaviour. Firstly, the tris(dpp) complex is surrounded by solvent molecules in the gel. The temperature-dependent emission data which seem to suggest a solvent melting range are in agreement with such an interpretation. It is however not clear why the compound would behave so differently especially when compared with $[Ru(bpy)(dpp)_2]^{2+}$. Secondly, it is possible that the excited-state properties of the tris(dpp) compound are

significantly different from those of the others in the series. If this is the case then it seems unlikely that an increase of the energy of the ^{3}MC level is the reason for the modified photophysics of the bpy-based complexes in the gel matrix. In that case the same behaviour would be expected for the tris(dpp) complex since it seems unlikely that there would be a substantial difference between the various compound in these energy levels and their behaviour with respect to incorporation in the solid matrix. Differences in the shape and horizontal position of the excited-state levels involved would appear to be a more likely explanation of the behaviour of the bpy-based complexes. Unfortunately RR measurements carried our for the tris(dpp) complex were inconclusive and we can not at present differentiate between the two possible models. Further experiments are in progress to clarify the situation.

However, it is clear from our study, that the excited-state properties of compounds observed in solution can not be transferred to the xerogel. These observations have important consequences for the application of such modified gels as oxygen sensors. For the optimisation of the sensor applications of such immobilised species a detailed analysis of the temperature dependence of the emitting properties is clearly beneficial. For example the compound $[Ru(dpp)_3]^{2+}$ is the preferred complex for oxygen sensing. However, our study suggests that for this complex population of the photoactive ^{3}MC state is observed and as a result the compound is intrinsically photolabile. Furthermore its emission lifetime is strongly temperature dependent. On the other hand the mixed bpy/dpp complexes are expected to be photostable and also have longer and virtually temperature-independent emission lifetimes. They seem therefore more suitable probes for oxygen sensing than the tris(dpp) complex. Also, if the explanation for the different emitting behaviour observed for the $[Ru(dpp)_3]^{2+}$ complex is that it is surrounded by solvent molecules rather than trapped within a solid cell, this might have implications for the design of oxygen sensors. Effective quenching by O_2 might be associated with a liquid environment. Finally, the results obtained are of interest for the design of luminescence based temperature sensors such as those reported by Demas and DeGraff.[44]

We gratefully acknowledge Forbairt and the EPSRC (Grant No GR/J01905) for financial support Johnson Matthey are thanked for a generous gift of $RuCl_3 \cdot xH_2O$.

References

1 T. J. Meyer, *Prog. Inorg. Chem*., 1983, **39**, 389.
2 K. R. Seddon, *Coord. Chem. Rev*., 1982, **41**, 79.
3 K. Kalyanasunduram, *Coord. Chem. Rev*., 1982, **41**, 159.
4 G. A. Crosby, G. D. Hager and R. J. Watts, *J. Am. Chem. Soc*., 1975, **97**, 7031.
5 S. R. Allsopp, A. Cox, S. H. Jenkins, S. Tunstal, T. J. Kemp and W. J. Reed, *J. Chem. Soc*., *Faraday Trans. 1*, 1978, **74**, 1275.
6 J. V. Houten and R. J. Watts, *J. Am. Chem. Soc*., 1976, **98**, 4853.
7 R. S. Lumpkin, E. M. Kober, L. A. Worl, Z. Murtaza and T. J. Meyer, *J. Phys. Chem*., 1990, **94**, 239.
8 B. Durham, J. V. Caspar, J. K. Nagle and T. J. Meyer, *J. Am. Chem. Soc*., 1982, **104**, 4803.
9 A. Juris, V. Balzani, F. Barigelletti, S. Campagna, P. Belser and A. Von Zelewsky, *Coord. Chem. Rev*., 1988, **84**, 85.
10 R. Matsui, S. Sasaki and N. Takahashi, *Langmuir*, 1991, **7**, 2866.
11 F. N. Castellano, T. A. Heimer, M. T. Tandahasetti and G. J. Meyer, *Chem. Mater*., 1994, **6**, 1041.
12 J. Fan and H. D. Gaffney, *J. Phys. Chem*., 1994, **98**, 13058.
13 B. Grass, O. Katz, J. Samuel, D. Avnir and M. Ottelenghi, *J. Phys. Chem*., 1995, **99**, 14893.
14 B. D. Macraith, C. McDonagh, G. O'Keeffe, E. T. Keyes, J. G. Vos, B. O'Kelly and J. F. McGilp, *Analyst*, 1993, **118**, 385.
15 P. Kiernan, C. McDonagh, B. D. MacCraith and K. Mongey, *J. Sol–gel Sci. Technol*., 1994, **2**, 513.
16 E. R. Carraway, J. N. Demas, B. A. DeGraff and J. R. Bacon, *Anal. Chem*., 1991, **63**, 337.
17 J. V. Caspar, and T. J. Meyer, *J. Am. Chem. Soc*., 1983, **105**, 5583.
18 R. J. Watts and G. A. Crosby, *J. Am. Chem. Soc*., 1971, **93**, 3184.
19 J. Baggot, G. Gregory, M. Piling, S. Anderson, K. Seddon and J. Turp, *J. Chem. Soc*., *Faraday Trans. 2*, 1983, **79**, 195.
20 E. M. Ryan, R. Wang, J. G. Vos, R. Hage and J. G. Haasnoot, *Inorg. Chim. Acta*, 1993, **208**, 49.
21 K. Mongey, C. M. McDonagh, B. D. MacCraith and J. G. Vos, *J. Sol–gel Sci. Technol*., 1997, **8**, 979.
21 H. Willard, *Instrumental Methods of Analysis*, Wadsworth, California, 7th edn., 1988.
22 J. N. Demas and G. A. Crosby, *J. Phys. Chem*., 1971, **75**, 991.
23 K. Makamura, *Bull. Chem. Soc. Jpn*., 1982, **55**, 2697.
24 R. Hage, PhD Thesis, Dublin City University, Dublin, 1991.
25 P. C. Alford, M. S. Cook and P. J. Robbins, *J. Chem. Soc*., *Perkin Trans. 2*, 1985, 705.
26 W. Wallace and P. Hoggard, *Inorg. Chem*., 1980, **19**, 2141.
27 R. A. Dellaguardia and J. K. Thomas, *J. Phys. Chem*., 1983, **87**, 990.
28 F. N. Castellano and G. J. Meyer, *J. Phys. Chem*., 1995, **99**, 14742.
29 S. Modes and P. Lianos, *Chem. Phys. Lett*., 1988, **4**, 351.
30 C. J. Brinker and J. Scherer, *Sol–gel Science: The Physics and Chemistry of Sol–gel Processing*, Boston, Academic Press, 1991.
31 K. Matsui K. Sasaki and N. Takahashi, *Langmuir*, 1991, **7**, 2866.
32 M. M. E. Severin-Vantilt and E. W. J. L. Oomen, *J. Non-Cryst. Solids*, 1993, **159**, 38.
33 R. Dallinger, W. Woodruff, P. Bradley, N. Kress and B. Hornberger, *J. Am. Chem. Soc*., 1981, **103**, 7441.
34 C. Kumar, J. Barton, I. Gould, N. Turro and J. Van Houten, *Inorg. Chem*., 1988, **27**, 648.
35 C. Kumar, J. Barton, I. Gould and N. Turro, *Inorg. Chem*., **1987**, 26, 1455.
36 H. Yersin and E. Galluber *J. Am. Chem. Soc*., 1984, **106**, 6582,.
37 M. Fetterolf and H. Offen, *J. Phys. Chem*., 1986, **90**, 1828.
38 M. Kasha and B. Dellinger, *Chem. Phys. Lett*., 1976, **38**, 9.
39 R. J. Watts and D. J. Missimer, *J. Am. Chem. Soc*., 1975, **100**, 5350.
40 E. M. Kober, J. V. Caspar, R. S. Lumpkin and T. J. Meyer, *J. Phys. Chem*., 1986, **90**, 3722.
41 K. Maruszewski and J. R. Kincaid, *Inorg. Chem*., 1995, **34**, 2002.
42 T. Kenelly, H. D. Gafney and M. Braun, *J. Am. Chem. Soc*., 1985, **107**, 4431.
43 A. W. Adamson, in *Inorganic Photochemistry*, Academic Press, New York, 1975, ch. 10.
44 J. N. Demas and B. A. DeGraff, *Proc. SPIE*, 1992, **1796**, 71.

Paper 7/01385J; *Received* 27*th February*, 1997